UNIVERSITY OF
WOLVERHAMPTON

Parameter estimation of the fractional-order Hammerstein–Wiener model using simplified refined instrumental variable fractional-order continuous time

Item Type	Journal article
Authors	Allafi, Walid;Zajic, Ivan;Uddin, Kotub;Burnham, Keith J.
Citation	Allafi, W., Zajic, I., Uddin, K., Burnham, KJ. (2017) 'Parameter estimation of the fractional-order Hammerstein–Wiener model using simplified refined instrumental variable fractional-order continuous time', IET Control Theory & Applications, 11 (15) pp. 2591-2598 doi: 10.1049/iet-cta.2017.0284
DOI	10.1049/iet-cta.2017.0284
Publisher	The Institution of Engineering and Technology
Journal	IET Control Theory & Applications
Download date	2025-05-23 11:48:42
License	https://creativecommons.org/licenses/by/3.0/
Link to Item	http://hdl.handle.net/2436/620762

IET Control Theory & Applications

Research Article

IET Journals
The Institution of Engineering and Technology

Parameter estimation of the fractional-order Hammerstein–Wiener model using simplified refined instrumental variable fractional-order continuous time

ISSN 1751-8644
Received on 21st March 2017
Revised 3rd June 2017
Accepted on 3rd July 2017
E-First on 9th August 2017
doi: 10.1049/iet-cta.2017.0284
www.ietdl.org

Walid Allafi[1,2] ✉, Ivan Zajic[2], Kotub Uddin[1], Keith J. Burnham[3]

[1]*WMG, The University of Warwick, Coventry CV4 7AL, UK*

[2]*School of Mechanical, Aerospace and Automotive Engineering, Faculty of Engineering, Environment and Computing, Coventry University, 10 Coventry Innovation Village, Coventry, CV1 2TL, United Kingdom*

[3]*Faculty of Science and Engineering, University of Wolverhampton, Wulfruna Street, Wolverhampton, WV1 1LY, United Kingdom*

✉ *E-mail: allafiw@gmail.com*

Abstract: This study proposes a direct parameter estimation approach from observed input–output data of a stochastic single-input–single-output fractional-order continuous-time Hammerstein–Wiener model by extending a well known iterative simplified refined instrumental variable method. The method is an extension of the simplified refined instrumental variable method developed for the linear fractional-order continuous-time system, denoted. The advantage of this novel extension, compared with published methods, is that the static output non-linearity of the Wiener model part does not need to be invertible. The input and output static non-linear functions are represented by a sum of the known basis functions. The proposed approach estimates the parameters of the linear fractional-order continuous-time subsystem and the input and output static non-linear functions from the sampled input–output data by considering the system to be a multi-input–single-output linear fractional-order continuous-time model. These extra inputs represent the basis functions of the static input and output non-linearity, where the output basis functions are simulated according to the previous estimates of the fractional-order linear subsystem and the static input non-linear function at every iteration. It is also possible to estimate the classical integer-order model counterparts as a special case. Subsequently, the proposed extension to the simplified refined instrumental variable method is considered in the classical integer-order continuous-time Hammerstein–Wiener case. In this paper, a Monte Carlo simulation analysis is applied for demonstrating the performance of the proposed approach to estimate the parameters of a fractional-order Hammerstein–Wiener output model.

1 Introduction

With ever decreasing product time-to-market and increasing cost of exhaustive testing, the modelling of complex systems has become an integral part of the product design cycle. Although in exceptional cases, a physical system exhibits linear behaviour, most physical systems exhibit non-linear characteristics [1]. Experimental and simulation studies have shown that the dynamic behaviour of non-linear systems can be significantly different from their linear counterparts [2–4]. As such, the development of techniques that facilitate the modelling of non-linear systems is paramount. In this regard, the vast body of current research in the field of non-linear dynamical systems has focused on non-linear systems identification and predicting non-linear system behaviour.

One class of such modelling systems is fractional-order systems [5–9] which employ fractional derivatives and integrals. Although fractional-order systems were introduced in the 18th century [10], research in this area has largely been restricted to the integer-order case due to insufficient computational resources [11]. Since the 1980s, as computing technology matured, the necessary tools to implement fractional-order systems for modelling, estimation and control were developed. Fractional-order systems have subsequently found wider applications in engineering, [12] physics [13, 14] and control [15, 16]. For example, the battery system is employed in energy storage applications and described by a fractional-order model, known as Randle's equivalent circuit (REC) [17]. It can be found that both branches of REC contain a constant phase element which is a different expression of the fractional-order integral. Furthermore, the Warburg element is also characterised by a fractional-order integral [17]. Fractional-order controllers are widely used for providing a robust control, for instance the fractional-order proportional integral derivative controller was shown to exhibit over the classical proportional integral derivative controller in an electro-hydraulic servo application [18], better response, better minimum performance indices values, better disturbance rejection, and better sinusoidal trajectory [19]. In the case of system identification, fractional calculus appears in the fractional least mean squares method which provides efficient performance in the pretense of active Box–Jenkins noise when estimating the parameters of linear and non-linear systems [20, 21]. Generally, there are advantages of applying the fractional-order representation over the integer-order representation, namely the ability for more robust control [22] and a wider performance range in aspects of modelling [11].

Another class of non-linear dynamical models is the so-called block-oriented models that consist of various configurations of linear dynamic blocks and non-linear memoryless blocks. The simplest examples in this class are cascaded systems with the non-linear block either preceding (Hammerstein model) or following (Wiener model) the linear block. There are several practical applications of the Hammerstein and Wiener formulations which are used to model systems with significant non-linearity in different fields. The Hammerstein model, for example, is employed in robotic therapy for describing the isometric recruitment curve, that is, the static gain relation between the stimulus activation level and steady-state output torque [23]. In the automotive industry, the battery impedance model is enhanced by introducing a Wiener static non-linearity to the ordinary equivalent circuit model [24]. Hammerstein models have also been employed to address bilinear models to represent the air handling unit of large heating ventilation and air conditioning systems [25], where it is principally used to describe the non-linearity introduced by the valves.

This is an open access article published by the IET under the Creative Commons Attribution License
(http://creativecommons.org/licenses/by/3.0/)

The model where a non-linear block both precedes and follows a linear dynamic system is called a Hammerstein–Wiener model [26, 27]. The advantages of the Hammerstein–Wiener class of models are (i) that the dynamics of systems are mainly generated by the linear subsystem, so that algorithms and techniques developed for the linear systems might be adopted for the Hammerstein–Wiener model case and (ii) if the static non-linearity has an inverse function, such that it allows for a cancellation with the static non-linearity, then linear control algorithms can be applied. In the context of real applications, this class of models have been exploited for modelling in various physical systems, for example, for radio frequency transmitters and power amplifiers [28], electrical muscle stimulation applications [29], magnetospheric and ionospheric systems [30], and agriculture [31], where Hammerstein–Wiener models assist in predicting the core temperature of silage stack-bales using wireless sensor networks.

The estimation approach of the Hammerstein–Wiener models can be either categorised as iterative or non-iterative. This work has primarily focused on the iterative methods. In the discrete-time domain, the iterative algorithm proposed in [32] is based on accessing the internal signals by using the key term separation principle as a decomposition technique. This algorithm was extended for the case of multi-inputs by Vörös in [33]. The approach adopted in [32, 33] expresses the Hammerstein and Wiener models linearly in parameters. The key term separation principle and estimated linear outputs, adopted in [32, 33], are also used in the case of the Wiener model in [34]. The principle drawbacks of this approach are namely that it is not a direct identification method and the convergence is not guaranteed. Other approaches for discrete iterative methods can be found in [35, 36]. In recent studies in the discrete domain, the kernel, Volterra, and fractional least mean square algorithms have been applied for estimating the parameters of the Hammerstein models associated with coloured noise process [37]. These approaches managed to estimate the parameters but it required a large number of iterations. The iteration number is shown to be reduced by employing the sliding-window approximation-based fractional least mean squares in [21] but still the iteration number is considerably large. All the aforementioned approaches are in the discrete-time domain and are employed for obtaining the continuous-time transfer function of the linear subsystem. A further step is required to convert from the discrete time to the continuous-time domain and this class of estimation approaches is termed indirect.

Garnier and Young summarised the advantages of the direct approaches over the indirect approaches in modelling as follows: (i) the continuous-time model identification offers a differential equation which is how most physical systems are mathematically represented, (ii) the continuous-time model parameter values often have physical meaning, (iii) these values are not a function of the sampling interval, hence eliminating the need for the conversion from discrete to continuous time that is an essential element of indirect approaches for estimating based on discrete-time models, (iv) direct continuous-time model estimation methods provide more efficient results in case of stiff systems, where a non-fixed sampling interval is required, and (v) the direct methods have proven successful in many practical applications. For the continuous-time domain, the refined instrumental variable method is a direct approach and is used to identify the Hammerstein–Wiener continuous-time model with the assumption of an invertible static non-linear function for the Wiener part. The parameters are obtained by applying singular value decomposition to the estimated multiple-inputs– single-output linear model which represents the whole non-linear model [38].

Advantages of both the Hammerstein–Wiener continuous-time models and the fractional-order continuous-time system models led to the introduction of the fractional-order continuous-time Hammerstein, Wiener, and Hammerstein–Wiener (HFC, WFC, and HWFC) models. In these formulations, the static non-linear functions are assumed to be described by a sum of the known basis functions. Parameter estimation is required when dealing with real-life practical applications, thus there have been proposals for iterative methods, termed simplified refined instrumental variable (SRIV), for HFC, WFC, and HWFC models which are abbreviated as HSRIVCF, WSRIVCF, and HWSRIVCF, respectively. The refined instrumental variable method for linear continuous-time systems was first proposed by Young and Jakeman [39] and extended for the fractional-order systems in [40]. It has also been successfully extended to estimate the parameters of the Hammerstein and Wiener models [38, 41] in which the static output non-linear function is assumed to be invertible [38].

In this paper, a direct parameter estimation approach from observed input–output data of a stochastic single-input– single-output fractional-order continuous-time Hammerstein–Wiener model by extending a well known iterative simplified refined instrumental variable method is proposed. The derivation of the proposed method is found to be similar to that of the simplified refined instrumental variable methods for multi-input– single-output linear fractional-order continuous-time systems. The approach proposed in this paper reformulates the non-linear HFC, WFC, and HWFC models to be described by multi-input, single-output linear fractional-order continuous-time models. The multi-input signals are the outputs of basis functions of the static non-linear functions whose inputs are the actual input of the static input non-linear function and the output of the estimated fractional-order continuous-time linear subsystem. The novelty of this paper stems from the use of the simulated linear subsystem output for obtaining the basis functions of the static output non-linear and extension to the case of fractional-order models.

This paper is organised as follows: the problem description for a fractional Hammerstein–Wiener model is introduced in Section 2. In Section 3, there is an illustration of the problem reformulation based on an HFC model. Section 4 shows the problem reformulation based on a WFC model. Both the HFC and WFC models are coupled in one model in the problem reformulation based on an HWFC model in Section 5 and identified by applying HWSRIVCF in Section 6. A numerical study on HWFC model identification is presented in Section 7. Finally, this paper concludes in Section 8.

2 Background to fractional-order systems

This section introduces the fundamental theory on which this paper is based, namely the theory of fractional-order derivatives, integrals, and their Laplace transform.

2.1 Fractional-order calculus

Fractional-order integral and derivative terms are generalised by fractional-order calculus. The term denoted ${}_a\mathscr{D}_t^\alpha$ is defined as:

$$ {}_a\mathscr{D}_t^\alpha = \begin{cases} \dfrac{\mathrm{d}^\alpha}{\mathrm{d}t^\alpha} & \alpha > 0 \\ 1 & \alpha = 0 \\ {}_a^t\mathscr{I}^{-\alpha} = \displaystyle\int_a^t \mathrm{d}t^{-\alpha} & \alpha < 0 \end{cases} \tag{1} $$

The operator $\mathscr{D}$ and the real number order α together represent the fractional-order term whether it is a derivative or integral. When the real number α is positive, it represents fractional-order derivative and when α is negative, it represents a fractional-order integral. In this paper, for retaining moderate complexity, the order α is considered to be a real number and always positive $\alpha \in \mathbb{R}^+$. Thus, in this paper, the terms for describing the fractional-order derivative and integral are $\mathscr{D}^\alpha$ and $\mathscr{I}^\alpha$, respectively.

2.1.1 Fractional-order integral.: The focus of this section is on Riemann–Liouville's conception which will later be used for the Laplace transform derivation. More detailed definitions are presented in [42]. The Riemann–Liouville definition is based on a consequence of Cauchy's formula for iterated integrals [43]

$$ {}_a^t\mathscr{I}^\alpha f(t) = \frac{1}{\Gamma(\alpha)} \int_a^t (t-\tau)^{\alpha-1} f(\tau)\,\mathrm{d}\tau, \quad \alpha \in \mathbb{R}^+ \tag{2} $$

This is an open access article published by the IET under the Creative Commons Attribution License (http://creativecommons.org/licenses/by/3.0/)

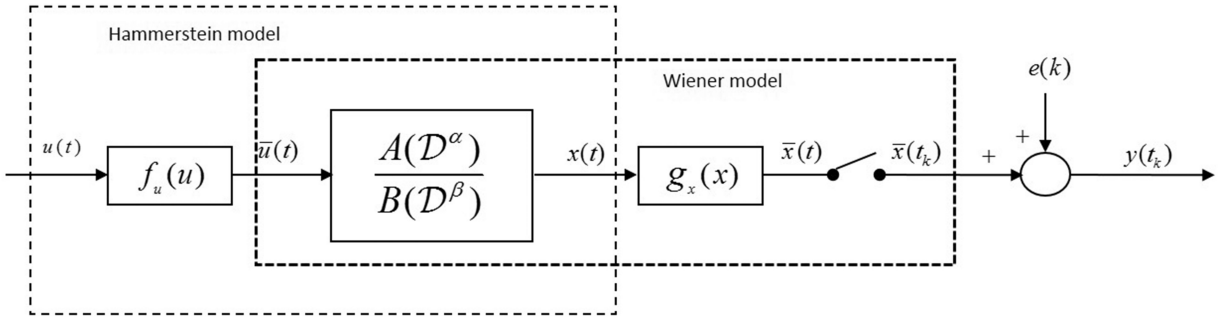

Fig. 1 *Block diagram of the Hammerstein–Wiener model processes*

where the Euler function is defined as

$$\Gamma(x) = \int_0^\infty t^{x-1}e^{-t}\,\mathrm{d}t \quad x \in \mathbb{R}\,. \tag{3}$$

If $a = 0$, it can be noted that the integral in (2) is a convolution of two signals $t^{\alpha-1}$ and $f(t)$. Therefore, (2) can be expressed as

$$I^\alpha f(t) = \frac{1}{\Gamma(\alpha)}[t^{\alpha-1} * f(t)] \tag{4}$$

2.1.2 Fractional-order derivative.: This section focuses on the Grünwald–Letnikov definition. A more detailed derivation of fractional-orders can be found in [42]. A discrete-time definition of the concept of fractional-order differentiation was defined by Grünwald–Letnikov based on the generalisation of the backward difference [44]

$$\mathcal{D}^\alpha f(t)\big|_{t=KT_\mathrm{s}} = \lim_{T_\mathrm{s}\to 0}\frac{1}{T_s^\alpha}\sum_{k=0}^{K}(-1)^k\binom{\alpha}{k}f((K-k)T_\mathrm{s}) \tag{5}$$

where $\binom{\alpha}{k}$ is the Newton's binomial function and T_s is the sampling interval. It is generalised using Euler's Gamma function and extended to fractional-order as

$$\binom{\alpha}{k} = \frac{\Gamma(\alpha+1)}{\Gamma(k+1)\Gamma(\alpha-k+1)} \tag{6}$$

It can be noted from (6) that the fractional-order derivative depends on all past data unless $\alpha \in \mathbb{Z}$. This is why the fractional-order derivative is known as long memory.

2.1.3 Laplace transform.: One of the most significant theories in control engineering is the Laplace transform of the linear fractional-order model. The Laplace transform of the fractional-order integral term can be derived from Riemann–Liouville's theory. The Laplace transform of the convolution in (4) can be expressed as

$$\begin{aligned}\mathscr{L}(I^\alpha f(t)) &= \mathscr{L}\left(\frac{t^{\alpha-1}}{\Gamma(\alpha)}\right)\mathscr{L}(f(t))\\ &= \frac{F(s)}{s^\alpha}\end{aligned} \tag{7}$$

where $\mathscr{L}(t^{\alpha-1}/\Gamma(\alpha)) = s^\alpha$ and $\alpha > 0$, see [45].

The Laplace transform of the fractional-order derivative of $f(t)$ can be obtained by [46]

$$\mathscr{L}(D^\alpha f(t)) = s^\alpha F(s) - \sum_{k=0}^{n-1}\left[s^k\frac{d^{\alpha-1-k}f(t)}{\mathrm{d}t^{\alpha-1-k}}\right]_{t=0} \tag{8}$$

where $\alpha \geq 0$ and $n \leq \alpha < n+1$. For simplicity, zero initial conditions are considered.

3 Problem description

A fractional-order continuous-time Hammerstein–Wiener model has static input and output (memoryless) non-linear functions, with an intermediate fractional-order continuous-time subsystem as illustrated in Fig. 1. The HWFC model can be described by the input–output relationship as follows:

$$\begin{aligned}\bar{u}(t) &= f_u(u(t))\\ x(t) &= \frac{B(\mathscr{D}^\beta)}{A(\mathscr{D}^\alpha)}\bar{u}(t)\\ \bar{x}(t) &= g_x(x(t))\\ y(t_k) &= \bar{x}(t_k) + e(k)\end{aligned} \tag{9}$$

where $u(t)$ and $\bar{u}(t)$ are the input and output of the static input non-linear function $f_u(u)$. The output of the static input non-linear function $\bar{u}(t)$ is the input of the fractional-order continuous-time linear subsystem whose output is $x(t)$ which becomes the input to the static output non-linear function, denoted $g_x(x)$ which generates $\bar{x}(t)$. The sampled form of $\bar{x}(t)$ at time instance k is denoted $\bar{x}(t_k)$, where $t = k \times T_\mathrm{s}$ and T_s is the sampling interval. Moreover, the last equation in (9) shows $y(t_k)$ is produced by corrupting $\bar{x}(t_k)$, with a discrete white (zero mean) noise denoted $e(k)$. The fractional-order continuous-time linear subsystem is described by a fractional-order differential equation in a form of the input and output polynomials, denoted $B(\mathscr{D}^\beta)$ and $A(\mathscr{D}^\alpha)$, respectively, and expressed as

$$\begin{aligned}A(\mathscr{D}^\alpha) &= a_0\mathscr{D}^{\alpha_n} + a_1\mathscr{D}^{\alpha_{n-1}} + \cdots + a_{n-1}\mathscr{D}^{\alpha_1} + a_n\\ B(\mathscr{D}^\beta) &= b_0\mathscr{D}^{\beta_m} + b_1\mathscr{D}^{\beta_{m-1}} + \cdots + b_{m-1}\mathscr{D}^{\beta_1} + b_m\end{aligned} \tag{10}$$

where the coefficients $a_j(j = 0, 1, \ldots n)$ and $b_j(j = 0, 1, \ldots m)$ are real constants, $\mathscr{D}^\alpha x(t) = \mathrm{d}^\alpha x(t)/\mathrm{d}t^\alpha$, $(\alpha_k(k = n, n-1, \ldots 1)) \in \mathbb{R}^+$, $(\beta_q(q = m, m-1, \ldots 1)) \in \mathbb{R}^+$, $\alpha_n > \alpha_{n-1}, \ldots > \alpha_1 > 0$, $\beta_m > \beta_{m-1} \ldots > \beta_1 > 0$ and $\alpha_n > \beta_m$ for physical feasibility. It is assumed that $a_0 = 1$ and the system is commensurate with base order, denoted α; therefore, $\alpha_i = \alpha \times i$ and $\beta_j = \alpha \times j$. Finally, it is assumed that the static non-linear functions are described by a sum of the basis functions and expressed as

$$\begin{aligned}\bar{u}(t) &= \sum_{j=1}^{r}\bar{b}_j f_j(u)\\ \bar{x}(t) &= \sum_{i=1}^{l}\bar{a}_i g_i(x)\end{aligned} \tag{11}$$

where the coefficients $\{\bar{a}_i, \bar{b}_j\} \in \mathbb{R}$, $(i = 1, \ldots, l)$, $(j = 1, \ldots, r)$.

4 Problem reformulation based on HFC model

In this paper, the static non-linear functions are individually treated as two different sub-models with a common linear subsystem for deriving the HSRIVCF and WSRIVCF methods. The HSRIVCF and WSRIVCF methods are then combined in an HWSRIVCF approach to identify the HWFC model.

This is an open access article published by the IET under the Creative Commons Attribution License
(http://creativecommons.org/licenses/by/3.0/)

If the HFC subsystem in (9) is separately treated, it is implied that the HFC model is formed of a cascade of the static input non-linear function and the linear fractional-time continuous-time subsystem, as shown in the left-hand dotted box in Fig. 1, corresponding to the first two equations in (9). It is assumed that the first parameter of the static input non-linear function is unity ($\bar{b}_1 = 1$). Since the basis function $f_i(u)$ is assumed to be a priori known and $u(t)$ is measurable, the basis functions can be time-dependent signals and denoted by, for simplicity, $\bar{f}_i(t)$. Under these conditions, the HFC subsystem can be described as a multi-input–single-output system

$$x(t) = \frac{B(\mathscr{D}^\beta)}{A(\mathscr{D}^\alpha)}\left(\bar{f}_1(t) + \sum_{i=2}^{r} \bar{b}_i \bar{f}_i(t)\right) \tag{12}$$

where

$$\bar{f}_i(t) = f_i(u) \tag{13}$$

Both the polynomial $B(\mathscr{D}^\beta)$ and the parameters of the static input non-linear function can be coupled to yield a vector of the over-parameterised input polynomial $\bar{B}_i(\mathscr{D}^\beta)$, where $\bar{B}_i(\mathscr{D}^\beta) = \bar{b}_i B(\mathscr{D}^\beta)$ and $\bar{B}_1(\mathscr{D}^\beta) = B(\mathscr{D}^\beta)$. Consequently (12) can be re-expressed in vector form as

$$x(t) = \frac{1}{A(\mathscr{D}^\alpha)}\left[\bar{B}(\mathscr{D}^\beta)\bar{F}(t)\right] \tag{14}$$

where the multi-input polynomial vector $\bar{B}(\mathscr{D}^\beta)$ and input vector $\bar{F}$ are given by

$$\bar{B}(\mathscr{D}^\beta) = \left[\bar{B}_1(\mathscr{D}^\beta), \quad \bar{B}_2(\mathscr{D}^\beta), \quad \ldots, \quad \bar{B}_r(\mathscr{D}^\beta)\right] \tag{15}$$

$$\bar{F}(t) = \left[\bar{f}_1(t), \quad \ldots, \quad \bar{f}_r(t)\right]^{\mathrm{T}} \tag{16}$$

5 Problem reformulation based on WFC model

This section illustrates how the WFC subsystem of the HWFC system in (9) is rearranged, so that any linear estimator can be employed. If the WFC subsystem of (9) is separately considered, it is realised as a cascade of the linear fractional-order continuous-time model and the static output non-linear function as shown in the right-hand bold dashed box in Fig. 1.

The parameter estimation is based on the collected input–output data.The input of the linear fractional-order continuous-time model is considered to be accessible in this section but its output is not accessible. It is assumed that the first basis function of the static output non-linear function in (11) is linear thus the static output non-linear function in (11) can be re-described as

$$\bar{x}(t) = x(t) + \sum_{i=2}^{l} \bar{a}_i g_i(x) \tag{17}$$

where $\bar{a}_1$ is normalised to unity and the basis functions of the static output non-linear functions $g_i(x)$, in the last term of (17), are considered to be known a priori. Therefore, they can be described by a function of time $\bar{g}_i(t) = g_i(x(t))$ if $x(t)$ is known. Thus, the $\bar{g}_i(t)$ functions are considered as inputs to the system. According to (9), (11), and (17), it is possible to characterise the WFC subsystem as a linear fractional-order continuous-time model with multi-input $(\bar{u}(t), \bar{g}_i(t))$ and single-output $\bar{x}(t)$ as

$$\bar{x}(t) = \frac{B(\mathscr{D}^\beta)}{A(\mathscr{D}^\alpha)}\bar{u}(t) + \sum_{i=2}^{l} \bar{a}_i \bar{g}_i(t) \tag{18}$$

6 Problem reformulation based on HWFC model

Both the reformulated HFC model in (15) and the WFC model in (18) are coupled by a linear fractional-order continuous-time subsystem in one equation, representing the noise-free HWFC model, given by

$$\bar{x}(t) = \frac{1}{A(\mathscr{D}^\alpha)}\bar{B}(\mathscr{D}^\beta)\bar{F}(t) + \sum_{i=2}^{l} \bar{a}_i \bar{g}_i(t) \tag{19}$$

where the over-parametrised polynomial $\bar{B}(\mathscr{D}^\beta)$ and vector $\bar{F}(t)$ are given in (15) and (16), with $\bar{g}_i(t) = g_i(x)$. Since measured data is used for parameter estimation, the output of the model in (19) is considered to be corrupted by a noise process. Thus, the HWFC model in (19) can be re-expressed as

$$y(t) = \bar{x}(t) + \xi(t) \tag{20}$$

where $y(t)$ is the noisy output and $\xi(t)$ represents the noise process.

7 HWSRIVCF method

Considering $\bar{g}_i(t)$ and $\bar{F}(t)$ to be inputs to the HWFC model, the model may thus be described by a multi-input, single-output linear fractional-order continuous-time model. The error functions of (19) and (20) are combined and expressed as

$$\varepsilon_{\mathrm{HW}}(t) = y(t) - \left(\frac{1}{A(\mathscr{D}^\alpha)}\bar{B}(\mathscr{D}^\beta)\bar{F}(t) + \sum_{i=2}^{l} \bar{a}_i \bar{g}_i(t)\right) \tag{21}$$

where the subscript *HW* refers to Hammerstein–Wiener.

Considering zero initial conditions, the Laplace transform of (21) is expressed as

$$E_{\mathrm{HW}}(s) = Y(s) - \left(\frac{1}{A(s^\alpha)}\bar{B}(s^\beta)\bar{F}(s) + \sum_{i=2}^{l} \bar{a}_i \bar{G}_i(s)\right) \tag{22}$$

which is reformulated such that the polynomial $A(s^\alpha)$ is associated with the noisy output $Y(s)$. This leads to the introduction of a filter $1/A(s^\alpha)$ in the first and second terms on the right-hand side of (22) for generating the filtered input–output data without filtering the error $E_{\mathrm{HW}}(s)$.

Therefore, (22) can be re-expressed as

$$E_{\mathrm{HW}}(s) = A(s^\alpha)\frac{1}{A(s^\alpha)}Y(s) - \left(\bar{B}(s^\beta)\frac{1}{A(s^\alpha)}\bar{F}(s) + \sum_{i=2}^{l} \bar{a}_i \bar{G}_i(s)\right) \tag{23}$$

Taking the inverse Laplace of (23) leads to

$$\begin{aligned}\varepsilon_{\mathrm{HW}}(t) = {} & A(\mathscr{D}^\alpha)\frac{1}{A(\mathscr{D}^\alpha)}y(t) \\ & - \left(\bar{B}(\mathscr{D}^\beta)\frac{1}{A(\mathscr{D}^\alpha)}\bar{F}(t) + \sum_{i=2}^{l} \bar{a}_i \bar{g}_i(t)\right)\end{aligned} \tag{24}$$

(24) can be then described in a filtered form by a model of the multi-input ($\bar{g}_i$, filtered $\bar{F}$), single filtered output form. Therefore, the error function (24) is rearranged and expressed as

$$\varepsilon_{\mathrm{HW}}(t) = A(\mathscr{D}^\alpha)y_{\mathrm{F}}(t) - \left(\bar{B}(\mathscr{D}^\beta)\bar{F}_{\mathrm{F}}(t) + \sum_{i=2}^{l} \bar{a}_i \bar{g}_i(t)\right) \tag{25}$$

where the filtered output and the vector of the filtered input are denoted $y_{\mathrm{F}}(t)$ and $\bar{F}_{\mathrm{F},B}(t)$, respectively, and the subscript F indicates the signal is filtered by $1/A(\mathscr{D}^\alpha)$. The filtered data can be obtained from

This is an open access article published by the IET under the Creative Commons Attribution License (http://creativecommons.org/licenses/by/3.0/)

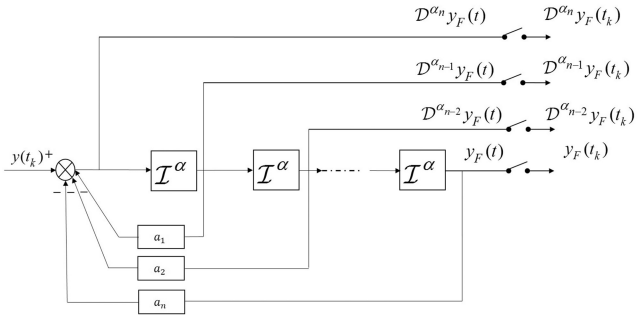

Fig. 2 *Equivalent block diagram of the state space representation of the filter* $1/A(\mathcal{D}^{\alpha})$ *shows how to generate the higher fractional-order derivative terms of the filtered signal* $y_F(t)$ *where* $\mathcal{I}^{\alpha} = \int_0^t \mathrm{d}t^{\alpha}$

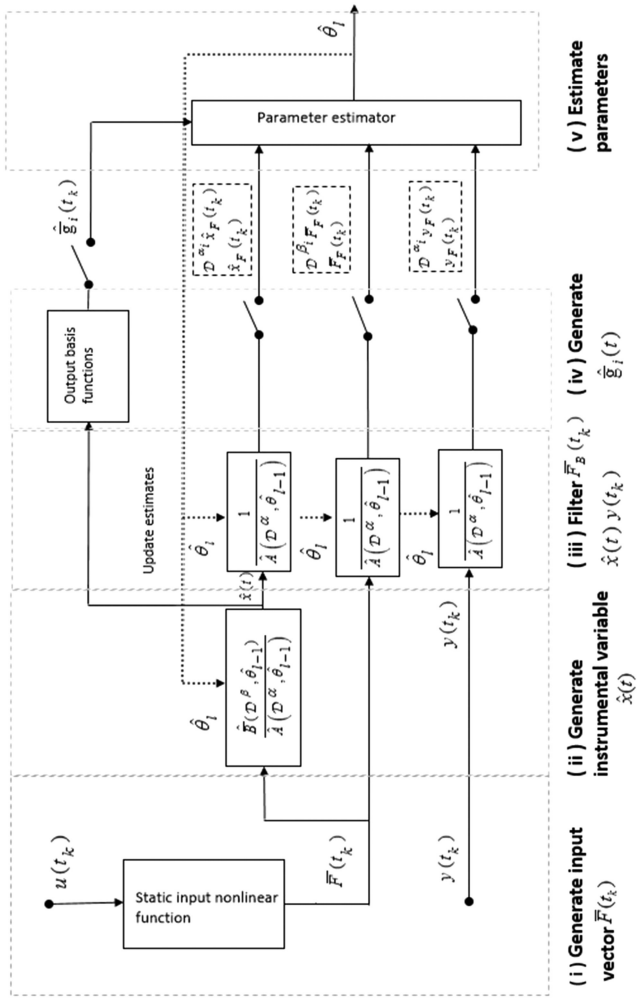

Fig. 3 *Iterative HWSRIVCF method processes*

$$\bar{F}_{\mathrm{F}}(t) = \frac{1}{A(\mathcal{D}^{\alpha})}\bar{F}(t_k)$$
$$y_{\mathrm{F}}(t) = \frac{1}{A(\mathcal{D}^{\alpha})}y(t_k) \tag{26}$$

Thus, the pseudo-regression form can be deduced based on sampled data of (25) and expressed as

$$\mathcal{D}^{\alpha_n} y_{\mathrm{F}}(t_k) = \varphi_{\mathrm{F}}^{\mathrm{T}}(t_k)\theta + \varepsilon(t_k) \tag{27}$$

where θ and $\varphi_F^{\mathrm{T}}(t_k)$ are given in [see (28), (29)], respectively

$$\theta = [a_1, \quad \cdots, \quad a_n, \quad \bar{b}_1 b_0, \quad \cdots, \quad \bar{b}_1 b_m, \quad \cdots, \quad \bar{b}_r b_0, \quad \cdots, \quad \bar{b}_r b_{m-1}, \quad \bar{b}_r b_m, \quad \bar{a}_2, \quad \cdots, \quad \bar{a}_l \tag{28}$$

(see (29)) .

All filtered terms in (29) can be readily obtained by implementing the equivalent block diagram of the state variable filter, as shown in Fig. 2, as a Simulink diagram.

There is an issue that $\bar{g}_i(t_k)$ is not accessible; however, $\bar{g}_i(t_k)$ can be simulated. Simulating $\bar{g}_i(t_k)$ requires the $\hat{B}(\mathcal{D}^{\beta})$, $\hat{A}(\mathcal{D}^{\alpha})$ polynomials and the estimated parameters of the static input non-linear function ($\hat{\bar{b}}_s$) to be available. In this paper, the initial $\hat{B}(\mathcal{D}^{\beta})$, $\hat{A}(\mathcal{D}^{\alpha})$ polynomials are selected according to three main factors which are (i) considering the output steady state of the linear system, (ii) considering whether the linear subsystem is under-damped or over-damped and (iii) the cut-off frequency which can be selected according to the fractional-order state variable filter design [47]. The selection of $\hat{\bar{b}}_s$ does not have a large influence on the estimation. For example, in the numerical example in this paper $\hat{\bar{b}}_s$ is selected such as $\hat{\bar{b}}_1 = \hat{\bar{b}}_2 = \hat{\bar{b}}_3 = 1$. An initial estimate of $\hat{A}(\mathcal{D}^{\alpha})$ is used for designing the filter $1/\hat{A}(\mathcal{D}^{\alpha})$. The parameters are then repeatedly estimated at every iteration as indicated by the subscript l, which represents the present iteration index. The HWSRIVCF method is iteratively implemented as illustrated in Fig. 3 and summarised as follows:

i. Compute the multi-input vector using the input static non-linear function $\bar{F}(t_k)$.

ii. Simulate the noise-free output $\hat{x}(t)$ using

$$\hat{x}(t) = \frac{1}{\hat{A}(\mathcal{D}^{\alpha}, \hat{\theta}_{l-1})}\hat{\bar{B}}(\mathcal{D}^{\beta}, \hat{\theta}_{l-1})_i \bar{F}(t_k) \tag{30}$$

where $\hat{x}(t)$ is used as the input to the static output non-linear function and as the instrumental variable.

iii. Filters $\hat{x}(t_k)$, $y(t_k)$, and $\bar{F}(t_k)$ to generate their filtered forms with their higher fractional-order derivatives, using

$$F(\mathcal{D}^{\alpha}) = \frac{1}{\hat{A}\left(\mathcal{D}^{\alpha}, \hat{\theta}_{l-1}\right)} \tag{31}$$

iv. Generate $\hat{\bar{g}}_i(t_k)$ in using $\hat{x}(t_k)$.

v. Obtain the estimated parameters using the instrumental variable least-square algorithm

$$\hat{\theta}_l = \left(\sum_{k=1}^{N} \hat{\varphi}_{\mathrm{F}}(t_k)\varphi_{\mathrm{F}}^{\mathrm{T}}(t_k)\right)^{-1} \sum_{k=1}^{N} \hat{\varphi}_{\mathrm{F}}(t_k)\mathcal{D}^{\alpha_n} y_{\mathrm{F}}(t_k) \tag{32}$$

where $\varphi_{\mathrm{F}}^{\mathrm{T}}$ is obtained from (29) and $\hat{\varphi}_{\mathrm{F}}$ is defined as (see (33)) .

vi. Repeat steps (i)–(iv) until the sum of the squares of the differences between $\hat{\theta}_{l-1}$and $\hat{\theta}_l$ is significantly small such as 10^{-4} or, for example, five iterations.

Whilst there would appear to be an issue associated with the estimates of the over-parameterised $\bar{B}(\mathcal{D}^{\beta})$ in (32), whereby $\bar{b}_s$ and b_s are combined within one vector, it was shown in [41] that $\bar{b}_s$ can be directly obtained from $B_i(\mathcal{D}^{\beta})$ in (32) by using

$$\varphi_{\mathrm{F}}^{\mathrm{T}}(t_k) = [-\mathcal{D}^{\alpha_n - 1} y_{\mathrm{F}}(t_k), \quad \cdots, \quad -y_{\mathrm{F}}(t_k), \quad \mathcal{D}^{\beta_m}\bar{f}_{\mathrm{F},1}(t_k), \quad \cdots, \quad \bar{f}_{\mathrm{F},1}(t_k), \quad \cdots, \quad \mathcal{D}^{\beta_m}\bar{f}_{\mathrm{F},r}(t_k), \quad \cdots, \quad \mathcal{D}^{\beta_1}\bar{f}_{\mathrm{F},r}(t_k), \quad \bar{f}_{\mathrm{F},r}(t_k), \quad \bar{g}_2(t_k), \quad \cdots, \quad \bar{g}_l(t_k)] \tag{29}$$

This is an open access article published by the IET under the Creative Commons Attribution License (http://creativecommons.org/licenses/by/3.0/)

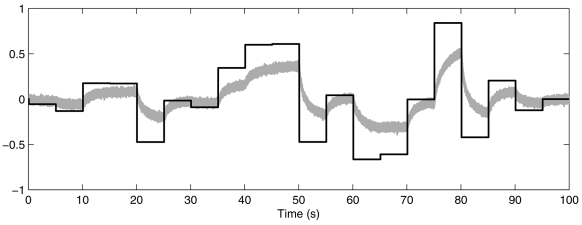

Fig. 4 *Random square wave input signal $u(t)$ and output signal $y(t)$ are presented in black and grey lines, respectively, when the* SNR = 20

$$\bar{b}_i = \frac{1}{m+1}\sum_{k=0}^{m}\frac{\hat{b}_{i,k}}{\hat{b}_{1,k}} \tag{34}$$

where $\hat{b}_{i,k}$ is the estimated form of $b_{i,k} = \bar{b}_i b_k$, given in (28).

7.1 Convergence of the algorithm

The convergence of the refined instrumental variable method was comprehensively analysed for the linear integer- order model in [48] and the integer order of Hammerstein–Wiener continuous-time model in [38], where the SRIV method is a special case of the refined instrumental variable method corresponding to a noise process sub-model $D(q) = C(q) = 1$. The instrumental variable is the noise-free output, similarly assumed in [38] and the reformulated structure(multi-input and single-output model) in (20) is the same structure as presented in [38]. The difference being that the system here is fractional and multi-input and single-output. This difference does not affect the proof, derived in [38]; therefore, those proofs, given in [38], are used here for formulating Theorem 1.

Theorem 1: Consider the algorithm (32) given by (28), (29), and, (33) and suppose the following assumptions exist.

Assumption 1: The true linear sub-system is asymptotically stable.

Assumption 2: The noise $e(k)$ is white (zero mean) and independent of the system input $u(t)$.

Assumption 3: $u(t)$ is produced such that the data set is sufficiently informative for the identification.

Then the following results are true.

Result 1: $E(\hat{\varphi}_{\mathrm{F}}(t_k)\varepsilon_{\mathrm{HW}}(t_k)) = 0$ where $E(\cdot) = \lim_{N\to\infty}(1/N)\sum_{k=1}^{N}(\cdot)$.

Result 2: $E(\hat{\varphi}_{\mathrm{F}}(t_k)\varphi_F^{\mathrm{T}}(t_k))$ is non-singular.

Proof: Only $\hat{x}(t_k) = x(t_k)$ is considered. In this condition, the error between the measured and noise free outputs is expressed as

$$\varepsilon_{\mathrm{HW}}(t_k) = e(t_k) \tag{35}$$

Result 1 is realised since all elements of $\hat{\varphi}_{\mathrm{F}}(t_k)$ are independent to the noise and the noise is white. The proof of Result 2 is presented in [38]. □

Therefore, the estimates in (32) can be obtained as $N \to \infty$. Further convergence analysis can be found in [38, 48]. The numerical study in this paper empirically shows that the estimates converge to the true parameters within the second to fifth iteration.

8 Numerical study

This section presents a numerical example to evaluate and highlight the performance of the proposed HWSRIVCF method for parameter estimation of an HWFC model. The static input non-linear function is described by a static polynomial form, i.e. $\bar{f}_i(t) = u^i$ and the output non-linear function is also represented by a static polynomial function. Thus, the HWFC model is given by

$$\begin{aligned}
\bar{u}(t) &= u(t) + \bar{b}_2 u^2(t) + \bar{b}_3 u^3(t)\\
x(t) &= \frac{b_0\mathscr{D}^{0.5} + b_1}{a_0\mathscr{D}^{1.5} + a_1\mathscr{D} + a_2\mathscr{D}^{0.5} + a_3}\bar{u}(t)\\
\bar{x}(t) &= x(t) + \bar{a}_2 x^2(t) + \bar{a}_3 x^3(t)\\
y(t_k) &= \bar{x}(t_k) + e(t_k)
\end{aligned} \tag{36}$$

The sampled input $\bar{u}(t_k)$ and the sampled noisy output $y(t_k)$ are collected and used for parameter estimation.

The system is simulated for 100 (s) with a fixed sampling interval of 10^{-3} (s). The selected Simulink solver is ode4 (Runge–Kutta). The fractional-order integral block is provided by the Fractional-Order Modeling and Control (FOMCON) Simulink library with frequency range [$0.001\,\mathrm{rad\,s^{-1}}$; $1000\,\mathrm{rad\,sc^{-1}}$] and an order approximation of 25. Details about the FOMCON Simulink library can be found in [49]. A square wave signal with a random amplitude is used as an input to the HWFC model, given in Fig. 4.

To evaluate the statistical performance of the proposed approach, a Monte Carlo simulation is performed for 50 runs. The same input signal is used for all runs but the white Gaussian noise is rearranged for different levels whilst keeping a fixed signal-to-noise ratio (SNR). The noise variance is selected such that the SNR = 10 and 20 dB, where SNR is defined in dB as

$$\mathrm{SNR} = 10\log\frac{P_{\bar{x}}}{P_e} \tag{37}$$

where $P_{\bar{x}}$ and P_e are the average power of the signals $\bar{x}$ and e, respectively.

It is assumed that the only accessible data is the input $u(t_k)$ and sampled noisy output $y(t_k)$, presented in Fig. 4. The system, considered for estimation using the HWSRIVCF method, is a multi-input [$\bar{f}_1(t_k)$, $\bar{f}_2(t_k)$, $\bar{f}_3(t_k)$, $\bar{g}_2(t_k)$, $\bar{g}_3(t_k)$] and single-output $y(t)$ model and expressed as

$$y(t) = \sum_{i=1}^{3}\frac{\bar{b}_i B(\mathscr{D}^{\beta})}{A(\mathscr{D}^{\alpha})}\bar{f}_i(t_k) + \bar{a}_2\hat{\bar{g}}_2(t) + \bar{a}_3\hat{\bar{g}}_3(t) + \varepsilon(t) \tag{38}$$

where $\hat{\bar{g}}_i(t) = \hat{\bar{x}}^i(t)$ but here $\hat{x}(t) = \sum_{i=1}^{3}((\hat{\bar{b}}_i\hat{B}(\mathscr{D}^{\beta},\hat{\theta}))/(\hat{A}(\mathscr{D}^{\alpha},\hat{\theta}))\bar{f}_i(t_k)$ and $\bar{f}_i(t_k) = u^i(t_k)$, and $\varepsilon(t)$ is the error due to the noise.

The initial input and output fractional-order linear polynomials are selected such that all roots $s_i^{0.5}$ are located at 1, hence $\hat{B}(\mathscr{D}^{\beta},\hat{\theta}_0) = \mathscr{D}^{0.5} + 1$ and $\hat{A}(\mathscr{D}^{\alpha},\hat{\theta}_0) = \mathscr{D}^{1.5} + 3\mathscr{D} + 3\mathscr{D}^{0.5} + 1$. The parameters of the static input non-linear function are selected to be unity, so that $\bar{b}_1 = \bar{b}_2 = \bar{b}_3 = 1$.

The results obtained from the Monte Carlo simulation analysis are presented in mean and standard deviations in Table 1. Table 1 demonstrates that the obtained results match the theory beyond the HWSRIVCF algorithm, where it gives unbiased estimates of the HWFC model parameters. Although the noise is relatively high, at the level of 10 dB, the proposed method converges. The standard deviations and the mean values obtained by HWSRIVCF are always correlated to the level of the measured noise. This means, in the case of the lower noise level (higher SNR), the mean value of the estimates converge more toward the true values and the standard deviations also decrease. Thus, the SNR significantly affects the convergence of the parameters to their true values.

The obtained results indicate that the parameter estimation errors associated with the static non-linear functions are lower

$$\begin{aligned}
\hat{\varphi}_{\mathrm{F}}^{\mathrm{T}}(t_k) = [&-\mathscr{D}^{\alpha_{n-1}}\hat{x}_{\mathrm{F}}(t_k), \quad \cdots, \quad -\hat{x}_{\mathrm{F}}(t_k) \quad \mathscr{D}^{\beta_m}\bar{f}_{\mathrm{F},1}(t_k), \quad \cdots, \quad \mathscr{D}^{\beta_0}\bar{f}_{\mathrm{F},1}(t_k)\\
&\cdots\mathscr{D}^{\beta_m}\bar{f}_{\mathrm{F},r}(t_k), \quad \cdots, \quad \mathscr{D}^{\beta_1}\bar{f}_{\mathrm{F},r}(t_k), \quad \mathscr{D}^{\beta_0}\bar{f}_{\mathrm{F},r}(t_k), \quad \hat{\bar{g}}_2(t_k), \quad \cdots, \quad \hat{\bar{g}}_l(t_k)]
\end{aligned} \tag{33}$$

This is an open access article published by the IET under the Creative Commons Attribution License (http://creativecommons.org/licenses/by/3.0/)

Table 1 Monte Carlo simulation results of parameter estimation of the HWCF system where $a_3 = \bar{a}_1 = \bar{b}_1$

SNR, dB		$a_0 = 1$	$a_1 = 3$	$a_2 = 2$	$b_0 = 1$	$b_1 = 0.5$	$\bar{a}_2 = 0.2$	$\bar{a}_3 = 0.6$	$\bar{b}_2 = 0.02$	$\bar{b}_3 = 0.25$
10	mean	1.1189	3.1563	2.1421	1.0927	0.4973	0.1988	0.6158	0.0219	0.2494
	standard	0.4083	0.5940	0.4760	0.3260	0.0129	0.0179	0.0854	0.0100	0.0165
20	mean	1.0096	3.0078	2.0101	1.0059	0.4999	0.1994	0.6015	0.0203	0.2499
	standard	0.1025	0.1530	0.1198	0.0824	0.0034	0.0045	0.0140	0.0027	0.0049

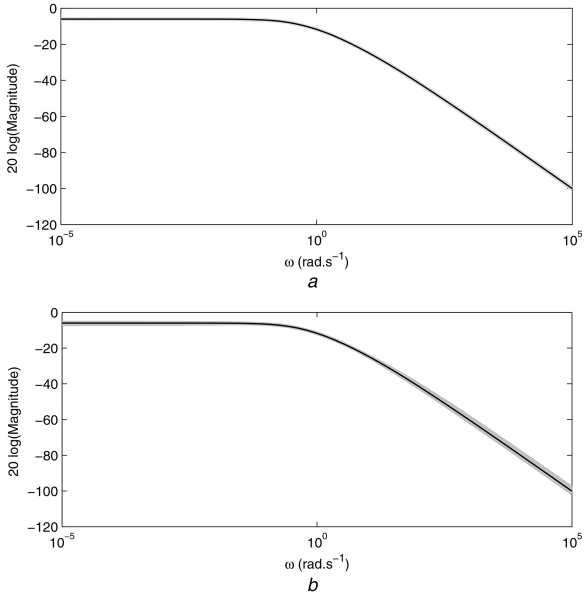

Fig. 5 *Magnitude Bode plots of actual and estimated linear submodel*
(a) For an SNR = 20 dB, ***(b)*** For an SNR = 10 dB

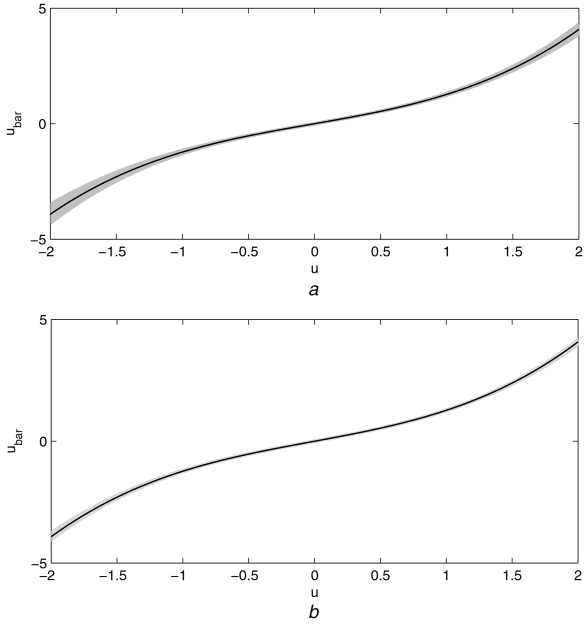

Fig. 6 *Input versus output of the actual and estimated static input non-linear function, given in the first equation in (9)*
(a) For an SNR = 20 dB, ***(b)*** For an SNR = 10 dB and u_{bar} is $\bar{u}$

when compared with the parameter estimation errors associated with the dynamic process. It should be emphasised that the parameter estimation errors of the static and dynamic sub-models of the overall Hammerstein–Wiener model are related via the error covariance matrix of the estimator (32). Nevertheless, the simulation results do indicate that the presented HWSRIVCF is statistically more efficient when estimating the static part of the overall Hammerstein–Wiener model. This observation is expected since the demand on having persistently exciting system input is somewhat more relaxed when estimating static functions as

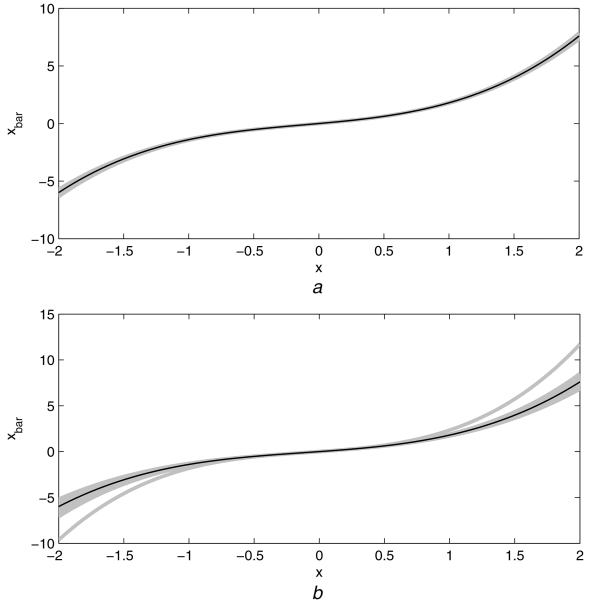

Fig. 7 *Input versus output of the actual and estimated static output non-linear function, given in the third equation in (9)*
(a) For an SNR = 20 dB, ***(b)*** For an SNR = 10 dB and x_{bar} is $\bar{x}$

opposed to dynamical processes. The error between the estimated and the actual outputs of the input and output static non-linear functions is small despite the existence of standard deviations of the estimates.

The empirical study of HWSRIVCF convergence is evaluated using the frequency response of the estimated HWFC models at each iteration for five iterations. Figs. 5*a*, *b*, 6*a*, *b*, and 7*a*, *b* show that the HWSRIVCF algorithm provides an almost perfect match to the true Bode plots for lower -noise level (higher SNR) in all iterations. These results agree with the results obtained using the ordinary simplified refined instrumental variable method, derived for estimating the parameters of a multi-input– single-output linear integer-order model and the integer-order Hammerstein–Wiener model, presented in [38, 50], respectively. In terms of the required number of iterations, the estimates are found to converge much quicker than the fractional-order least mean square-based techniques proposed, for example, in [21, 37] which considered the coloured noise processes.

9 Conclusions

The wide applicability of fractional-order models to replicate the non-linear phenomena exhibited in many practical systems is acknowledged. In this, motivated by historical applications of integer-order Hammerstein–Wiener models, stochastic single-input– single-output fractional-order continuous-time Wiener and Hammerstein–Wiener (WFC and HWFC, respectively) model structures are introduced. The HWFC model structure is characterised by a cascade connection of non-linear static functions transforming the input and output signals of a fractional-order continuous-time dynamic model. The static non-linear functions are represented by a combination of basis functions.

Prompted by the advantages WFC and HWFC models, this paper has proposed a new algorithm specifically developed for estimating the parameters of fractional-order non-linear models in the form of the HWFC model. The new algorithm is an extension of the simplified refined instrumental variable approach developed

This is an open access article published by the IET under the Creative Commons Attribution License
(http://creativecommons.org/licenses/by/3.0/)

for continuous-time integer-order linear models parameter estimation. It has shown how the algorithm is formulated and developed within the context of Hammerstein–Wiener model. This is achieved by describing the fractional-order continuous-time Hammerstein–Wiener model with a multi-input– single-output fractional-order system. The major advantage of the proposed approach is that the output static non-linear function does not need to be invertible.

Following the instrumental variable approach, the initialisation process does not have a large impact on the parameters convergence and the number of iterations required for convergence. The effectiveness of the proposed approach has been evaluated when applied to an arbitrary non-linear system in the presence of noisy output data via a Monte Carlo simulation study.

For future work, an extension of the proposed approach can be done to cope with a Box–Jenkins model. Furthermore, given that in most dynamical applications, model parameters vary with time, there is a requirement to update model parameters to cope with change in the dynamics. It is of benefit, therefore, to study the online formulation of the HWSRIVCF model.

10 Acknowledgments

This research was supported by EPSRC grants (EP/M507143/1) and (EP/N001745/1).

11 References

[1] Nelles, O.: '*Nonlinear system identification: from classical approaches to neural networks and fuzzy models*' (Springer Science & Business Media, 2013)

[2] Petrov, E., Ewins, D.: 'State-of-the-art dynamic analysis for non-linear gas turbine structures', *Proc. Inst. Mech. Eng. G, J. Aerosp. Eng.*, 2004, **218**, (3), pp. 199–211

[3] Goege, D.: 'Fast identification and characterization of nonlinearities in experimental modal analysis of large aircraft', *J. Aircr.*, 2007, **44**, (2), pp. 399–409

[4] Hunt, K.: 'Classification by induction: application to modelling and control of non-linear dynamical systems', *Intell. Syst. Eng.*, 1993, **2**, (4), pp. 231–245

[5] Bagley, R.L., Calico, R.: 'Fractional order state equations for the control of viscoelastically damped structures', *J. Guid. Control Dyn.*, 1991, **14**, (2), pp. 304–311

[6] Makroglou, A., Miller, R.K., Skaar, S.: 'Computational results for a feedback control for a rotating viscoelastic beam', *J. Guid. Control Dyn.*, 1994, **17**, (1), pp. 84–90

[7] Idiou, D., Charef, A., Djouambi, A.: 'Linear fractional order system identification using adjustable fractional order differentiator', *IET Signal Process.*, 2014, **8**, (4), pp. 398–409

[8] Narang, A., Shah, S.L., Chen, T.: 'Continuous-time model identification of fractional-order models with time delays', *IET Control Theory Appl.*, 2011, **5**, (7), pp. 900–912

[9] Yang, H., Jiang, B.: 'Stability of fractional-order switched non-linear systems', *IET Control Theory Appl.*, 2016, **10**, (8), pp. 965–970

[10] Ross, B.: 'The development of fractional calculus 1695–1900', *Historia Math.*, 1977, **4**, (1), pp. 75–89

[11] Monje, C.A., Chen, Y., Vinagre, B.M., et al.: '*Fractional-order systems and controls: fundamentals and applications*' (Springer Science & Business Media, 2010)

[12] Gutiérrez, R.E., Rosário, J.M., Tenreiro, Machado J.: 'Fractional order calculus: basic concepts and engineering applications', *Math. Probl. Eng.*, 2010, **2010**

[13] Hilfer, R.: 'Fractional diffusion based on Riemann–Liouville fractional derivatives', *J. Phys. Chem. B*, 2000, **104**, (16), pp. 3914–3917

[14] Zhao, Y., Baleanu, D., Cattani, C., et al.: 'Maxwell's equations on cantor sets: a local fractional approach', *Adv. High Energy Phys.*, 2013, **2013**

[15] Sierociuk, D., Dzielinski, A.: 'Fractional Kalman filter algorithm for the states, parameters and order of fractional system estimation', *Int. J. Appl. Math. Comput. Sci.*, 2006, **16**, (1), p. 129

[16] Allafi, W., Zajic, I., Burnham, K.J.: '*Identification of fractional order models: application to 1D solid diffusion system model of lithium ion cell*' (Springer International Publishing, Cham, 2015), pp. 63–68

[17] Buller, S., Thele, M., Karden, E., et al.: 'Impedance-based non-linear dynamic battery modeling for automotive applications', *Chin. J. Power Sources*, 2003, **113**, (2), pp. 422–430, proceedings of the International Conference on Lead-Acid Batteries, {LABAT} '02

[18] Essa, M., Aboelela, M., Hassan, M.: 'Application of fractional order controllers on experimental and simulation model of hydraulic servo system' in Azar, A.T., *et al.* (Eds.): '*Fractional order control and synchronization of chaotic systems*' (Springer, 2017), pp. 277–324

[19] Azar, A., Vaidyanathan, S., Ouannas, A.: '*Fractional order control and synchronization of chaotic systems*', vol. **688** (Springer, 2017)

[20] Raja, M., Chaudhary, N.: 'Adaptive strategies for parameter estimation of Box–Jenkins systems', *IET Signal Process.*, 2014, **8**, (12), pp. 968–980

[21] Aslam, M., Chaudhary, I., Raja, Z.: 'A sliding-window approximation-based fractional adaptive strategy for Hammerstein nonlinear armax systems', *Nonlinear Dyn.*, 2017, **87**, (1), pp. 519–533

[22] Sabatier, J., Lanusse, P., Melchior, P., et al.: '*Fractional order differentiation and robust control design: CRONE, H-infinity and motion control*', vol. **10** (Springer, 2015)

[23] Xu, W., Chu, B., Rogers, R.E.: 'Iterative learning control for robotic-assisted upper limb stroke rehabilitation in the presence of muscle fatigue', *Control Eng. Pract.*, 2014, **31**, pp. 63–64

[24] Widanage, W., Barai, A., Chouchelamane, G., et al.: 'Design and use of multisine signals for li-ion battery equivalent circuit modelling. part 2: model estimation', *Chin. J. Power Sources*, 2016, **324**, pp. 61–69

[25] Zajic, I., Larkowski, T., Sumislawska, M., et al.: 'Modelling of an air handling unit: a Hammerstein-bilinear model identification approach'. 2011 21st Int. Conf. Systems Engineering, 2011, pp. 59–63

[26] Wills, A., Schön, T.B., Ljung, L., et al.: 'Identification of Hammerstein–Wiener models', *Automatica*, 2013, **49**, (1), pp. 70–81

[27] Schoukens, J., Nemeth, J.G., Crama, P., et al.: 'Fast approximate identification of nonlinear systems', *Automatica*, 2003, **39**, (7), pp. 1267–1274

[28] Taringou, F., Hammi, O., Srinivasan, B., et al.: 'Behaviour modelling of wideband RF transmitters using Hammerstein–Wiener models', *IET Circuits Devices Syst.*, 2010, **4**, (4), pp. 282–290

[29] Bai, E.W., Cai, Z., Dudley-Javorosk, S., et al.: 'Identification of a modified Wiener–Hammerstein system and its application in electrically stimulated paralyzed skeletal muscle modeling', *Automatica*, 2009, **45**, (3), pp. 736–743

[30] Palanthandalam-Madapusi, H.J., Ridley, A.J., Bernstein, D.S.: 'Identification and prediction of ionospheric dynamics using a Hammerstein–Wiener model with radial basis functions'. American Control Conf., 2005, Proc. 2005, 2005, vol. **7**, pp. 5052–5057

[31] Nadimi, E.S., Green, O., Blanes-Vidal, V., et al.: 'Hammerstein–Wiener model for the prediction of temperature variations inside silage stack-bales using wireless sensor networks', *Biosyst. Eng.*, 2012, **112**, (3), pp. 236–247

[32] Vörös, J.: 'An iterative method for Hammerstein–Wiener systems parameter identification', *J. Electr. Eng.*, 2004, **55**, (11-12), pp. 328–331

[33] Vörös, J.: 'Parameter identification of Wiener systems with multisegment piecewise-linear nonlinearities', *Syst. Control Lett.*, 2007, **56**, (2), pp. 99–105

[34] Zhou, L., Li, X., Pan, F.: 'Least-squares-based iterative identification algorithm for Wiener nonlinear systems', in Hui-Shen, Shen (Ed.): '*IMA J. Appl. Math.*, 2013, **2013**

[35] Wang, D., Ding, F.: 'Least squares based and gradient based iterative identification for wiener nonlinear systems', *Analog Integr. Circuits Signal Process.*, 2011, **91**, (5), pp. 1182–1189

[36] Chen, H.T., Hwang, S.H., Chang, C.T.: 'Iterative identification of continuous-time Hammerstein and Wiener systems using a two-stage estimation algorithm', *Ind. Eng. Chem. Res.*, 2009, **48**, (3), pp. 1495–1510

[37] Chaudhary, N., Raja, M.: 'Identification of Hammerstein nonlinear armax systems using nonlinear adaptive algorithms', *Nonlinear Dyn.*, 2015, **79**, (2), pp. 1385–1397

[38] Ni, B., Gilson, M., Garnier, H.: 'Refined instrumental variable method for Hammerstein–Wiener continuous-time model identification', *IET Control Theory Appl.*, 2013, **7**, (9), pp. 1276–1286

[39] Young, P.C., Jakeman, A.: 'Refined instrumental variable methods of time series analysis: part iii, extensions', *Int. J. Control*, 1980, **31**, (4), pp. 741–764

[40] Allafi, W., Burnham, K.J.: 'Identification of fractional-order continuous-time hybrid Box–Jenkins models using refined instrumental variable continuous-time fractional-order method'. Advances in Systems Science – Proc. Int. Conf. Systems Science, 2013, pp. 785–794

[41] Laurain, V., Gilson, M., Garnier, H., et al.: 'Refined instrumental variable methods for identification of Hammerstein continuous-time Box–Jenkins models'. 47th IEEE Conf. Decision and Control, CDC'08, 2008, pp. 210–216

[42] Ortigueira, M.D.: '*Fractional calculus for scientists and engineers*' (Springer Science & Business Media, 2011)

[43] Oldham, K., Spanier, J.: '*The fractional calculus theory and applications of differentiation and integration to arbitrary order*', vol. **111** (Elsevier, 1974)

[44] Das, S.: '*Functional fractional calculus*' (Springer Science & Business Media, 2011)

[45] Schiff, J.: '*The Laplace transform*' (Springer Verlag, New York, 1999)

[46] Podlubny, I.: '*Fractional differential equations: an introduction to fractional derivatives, fractional differential equations, to methods of their solution and some of their applications*' (Academic Press, 1998)

[47] Cois, O., Oustaloup, A., Poinot, T., et al.: 'Fractional state variable filter for system identification by fractional model'. Control Conf. (ECC), 2001 European IEEE, 2001, 2001, pp. 2481–2486

[48] Liu, X., Wang, J., Zheng, W.X.: 'Convergence analysis of refined instrumental variable method for continuous-time system identification', *IET Control Theory Appl.*, 2011, **5**, (7), pp. 868–877

[49] Tepljakov, A., Petlenkov, E., Belikov, J.: 'Fomcon: fractional-order modeling and control toolbox for MATLAB'. Proc. 18th Int. Mixed Design Conf. Integrated Circuits and Systems, 2011, pp. 684–689

[50] Garnier, H., Gilson, M., Young, P., et al.: 'An optimal {IV} technique for identifying continuous-time transfer function model of multiple input systems', *Control Eng. Pract.*, 2007, **15**, (4), pp. 471–486

This is an open access article published by the IET under the Creative Commons Attribution License (http://creativecommons.org/licenses/by/3.0/)